Existence of basal oxygen vacancies on the rutile TiO_2 (110) surface

Katsuyuki Matsunaga,[1,2] Yusuke Tanaka,[1] Kazuaki Toyoura,[1] Atsutomo Nakamura,[1] Yuichi Ikuhara,[2,3] and Naoya Shibata[3,4]
[1]*Department of Materials Science and Engineering, Nagoya University, Furo-cho, Chikusa-ku, Nagoya 464-8603, Japan*
[2]*Nanostructures Research Laboratory, Japan Fine Ceramic Center, 2-4-1 Mutsuno, Atsuta-ku, Nagoya 456-8587, Japan*
[3]*Institute of Engineering Innovation, School of Engineering, the University of Tokyo, Yayoi 2-11-16, Bunkyo-ku, Tokyo 113-8656, Japan*
[4]*Japan Science and Technology Agency, PRESTO, 4-1-8 Honcho Kawaguchi, Saitama 332-0012, Japan*
(Received 27 December 2013; revised manuscript received 27 July 2014; published 10 November 2014)

On a rutile TiO_2 (110) surface, vacancies at the bridging oxygen sites are thought to be major surface point defects and strongly influence the surface phenomena. Using systematic density functional theory (DFT) calculations, however, we show that vacancies at the basal oxygen sites have comparable formation energies to the bridging oxygen vacancies. The correction of self-interaction error for localized Ti 3*d* states in DFT plays an important role for correctly describing the relative stability of the oxygen vacancies as well as the electronic structures. This new type of stable surface oxygen vacancy can be formed with a similar amount of the bridging oxygen vacancy in a relatively dilute condition, which may affect atom deposition and chemical reactions on the surface.

DOI: 10.1103/PhysRevB.90.195303 PACS number(s): 68.47.Gh, 61.72.jd

A rutile TiO_2 (110) surface has been commonly used as a model for fundamental research in the fields of surface science and catalysis for many years [1–3]. Atomic structures of the surfaces with metal atoms and molecules as well as that of the clean bare surface were well characterized by using scanning tunneling microscopy (STM), atomic force microscopy (AFM), and more recently, scanning transmission electron microscopy (STEM) [1–4]. The atomic structure of the stoichiometric clean (110) surface contains bridging oxygen atoms (O_{br}) arranging along the [001] direction (see Fig. 1). Here, O_{br} atoms are bonded to two underlying sixfold coordinated Ti atoms (Ti_{6c}), and are located at atomic sites protruding from the basal (110) atomic plane including three atomic species of Ti_{6c}, fivefold coordinated Ti atoms (Ti_{5c}), and basal threefold coordinated oxygen atoms (O_{ba}). It is also established that the (110) surface includes some amount of point defects, typically oxygen vacancies. This is because surface oxygen atoms are easily removed by thermal annealing or by sputtering in vacuum. Although the surface oxygen vacancy concentration is considered to be in the order of several percent from experimental spectroscopic analyses [3,5], oxygen vacancies on the surface strongly influence the surface reactivity. Therefore, it is essential to explore the nature of surface oxygen vacancies on the rutile surface and its relationship with TiO_2 properties.

So far, two types of oxygen vacancy sites on the surface were proposed experimentally. One is a vacancy at the bridging oxygen site [$V(O_{br})$], which is widely accepted as a major point defect species of the TiO_2 (110) surface. It has been reported that such bridging oxygen vacancies play an important role in noble metal atom adsorption (such as Au) [3,6–7], dissociation of water molecules [8–9], etc. In fact, almost all of the first-principles and the related density functional theory (DFT) calculations of the TiO_2 (110) surface done to reveal mechanisms of the surface phenomena, also often take account of the presence of $V(O_{br})$ as a major point defect on the surface. In contrast, the presence of oxygen vacancies in the subsurface layer below Ti_{5c} [$V(O_{sub})$] was suggested by Diebold *et al.* [10] based on their observed STM images. However, it is still unclear whether $V(O_{sub})$ is valid and involved in the real surface because no further experimental data was reported on this type of oxygen vacancy. Although this surface has been extensively studied both experimentally and theoretically, little is known about oxygen vacancies on the surface, except for $V(O_{br})$.

In this paper, we present theoretical results to show that oxygen vacancies at basal oxygen sites [$V(O_{ba})$], which is a type of stable surface oxygen vacancy, can exist on the TiO_2 (110) surface. In general, formation energies of neutral oxygen vacancies on the surface obtained from DFT calculations are dependent on sizes of surface slab models and thus suffer from a finite supercell size effect [11]. Larger sized surface slab models minimize the supercell size effect and provide intrinsic formation energies of oxygen vacancies on the surface. Moreover, there is a limitation of normal DFT calculation in describing the electronic structures of oxygen vacancies in TiO_2, which mainly arises from the self-interaction error [12]. From systematic calculations with different supercell sizes and with/without self-interaction correction, it is found that the basal oxygen vacancy can be formed and has similar thermodynamic stability with the well-known bridging oxygen vacancy. Since oxygen vacancies are thought to affect adsorption and reactions of atoms and molecules on the surface, the presence of this new type of oxygen vacancy would become a key factor to explore unresolved phenomena on the TiO_2 (110) surface.

Technical details of this study are as follows. Density functional theory calculations are performed based on the projector-augmented wave (PAW) method within the generalized gradient approximation (GGA), implemented on Vienna *Ab initio* Simulation Package (VASP) [13–14]. The Perdew-Burke-Ernzerhof (PBE) GGA functional is used for exchange-correlation interactions between electrons [15]. Additionally, onsite Coulomb repulsion is taken into account with an effective U parameter only for Ti 3*d* electrons. This is because normal GGA calculations have a limitation describing localized *d* states due to the self-interaction error of GGA functionals. To correct this, the value of $U = 5.8$ eV is used here because this can properly describe defects in TiO_2 systems [16]. As an alternative approach, hybrid functional calculations

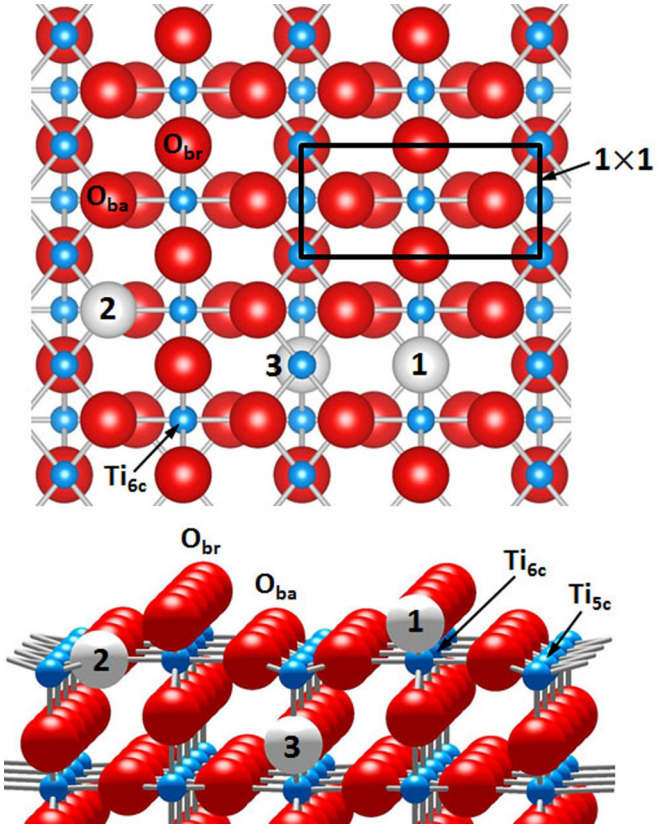

FIG. 1. (Color online) Atomic structure of the rutile TiO_2 (110) surface. The 1×1 surface unit is depicted by the rectangle in the upper figure. The numbered gray balls display the positions of oxygen vacancies (1: bridging site, 2: basal site, 3: subsurface site) considered in this paper.

may be used, but they are generally demanding and are difficult to apply to rather large supercells used in the present paper. As pointed out by Morgan and Watson [17], an appropriate U parameter of more than 4.2 eV can provide a reasonable description of the characteristic wave function originating from an oxygen vacancy on the TiO_2 surface. Wave functions are expanded by plane waves up to an energy cutoff of 500 eV throughout the present paper.

Neutral oxygen vacancies on the TiO_2 (110) surface are calculated by periodic surface slab models involving the (110) surfaces at both ends of the slab. The repeated surface slab models are separated by vacuum layers of more than 1.4 nm thickness to prevent spurious interactions between the surfaces. Neutral oxygen vacancies are introduced at the bridging [$V(O_{br})$] and basal oxygen sites [$V(O_{ba})$] of the slab surfaces and at the subsurface oxygen site [$V(O_{sub})$] just below Ti_{5c} (see Fig. 1), so as to make the surface slab symmetric. A slab thickness is also taken to be more than 2.2 nm (more than seven trilayers of O-Ti_2O_2-O). This is determined to be much larger than the interdefect distance parallel to the surface plane, which is related to the lateral size of the surface supercells as described below. It is noted that the surface slab models undergo the odd-even oscillation of adsorption energies of molecules with respect to the number of O-Ti_2O_2-O trilayers in the surface slab [18–19]. On the basis of water adsorption on this surface by Kowalski *et al.* [19], although the adsorption energy exhibits the odd-even oscillation, relative energies of different adsorption models (molecular and dissociative adsorption in their work) converge well to less than 0.1 eV in the slab thickness of more than seven trilayers. In addition, it was also confirmed in the present paper that test calculations for the surface slabs (2×4) with odd trilayers (from five to nine) show a good convergence of formation energies of a few tens of millielectron volts. These results ensure the validity of the relative stability of different types of oxygen vacancies on this surface calculated in the present paper.

The minimum surface unit of 1×1 for rutile TiO_2 (110) (see Fig. 1) is extended to 1×2 (doubled toward [001]), 2×4, and 3×6, to investigate the finite supercell size effect. Atomic positions in the individual supercells are allowed to relax until their forces are converged to 0.01 eV/Å. Brillouin-zone sampling is performed using a $4 \times 2 \times 1$ Monkhorst-Pack (MP) meshes for the 1×1 surface supercell, and MP meshes are reduced more appropriately for larger supercells, so as not to degrade computational accuracy. For comparison, oxygen vacancies in bulk rutile TiO_2 are also calculated by using differently sized bulk supercells.

Formation energies of neutral oxygen vacancies are evaluated from total energies of supercells with or without the oxygen vacancies. In this case, an atomic chemical potential of oxygen, which is necessary to evaluate the formation energies, is assumed to be equal to a total energy of an isolated O_2 molecule, corresponding to an oxidized condition. Of course, quantitative values of the defect formation energies depend on the oxygen chemical potential in a given chemical environment (such as partial pressure and temperature), but further detailed consideration is not explicitly made here, and relative stability of the possible surface defects will be discussed.

Figure 2(a) shows calculated formation energies of neutral oxygen vacancies in bulk and on the surface, plotted against the inverse of the average interdefect distance L^{-1}. Athough the calculated formation energies are obtained from the finite sized supercells, this plot can predict the formation energies

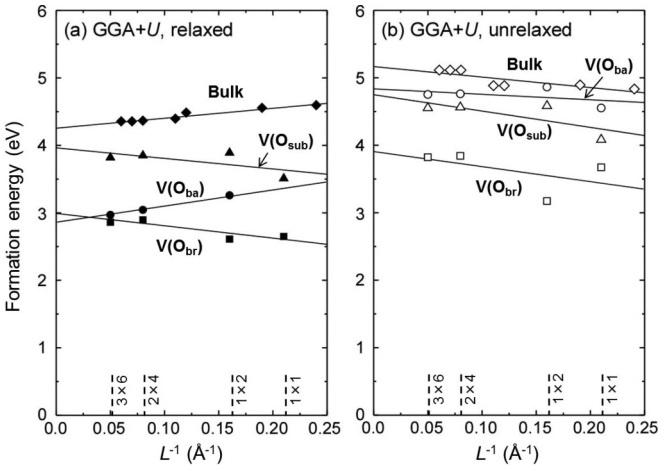

FIG. 2. Calculated formation energies of neutral oxygen vacancies by GGA + U ($U = 5.8$ eV) against an inverse of average interdefect distance L^{-1}. (a) Those obtained with structural relaxation; (b) those without relaxation.

in the dilute limit (without spurious interactions between the defects in the periodic finite supercells) from extrapolation of linear fitting of the calculated values to $L = \infty$ [11].

It can be seen from Fig. 2(a) that the formation energies of oxygen vacancies on the surface have smaller values than those in bulk over the entire range of L^{-1}. Among the vacancies on the surface, $V(O_{sub})$ exhibits a larger formation energy. The previous GGA calculations without the U correction by Cheng and Selloni [20] showed the larger formation energy of $V(O_{sub})$ by about 1.5 eV, as compared with that of $V(O_{br})$. Such a trend was also confirmed by our GGA results, which will be shown later. It is unlikely, therefore, that $V(O_{sub})$ is easily formed on this surface. Instead, $V(O_{br})$ and $V(O_{ba})$ exhibit smaller formation energies. Here, $V(O_{br})$ is most stable in the relatively larger L^{-1} range, which is consistent with the well-accepted view that $V(O_{br})$ is a major point defect on this surface. However, it is noteworthy to mention that $V(O_{ba})$ exhibits a similar formation energy with $V(O_{br})$ in the 3×6 surface slab (only the difference of 0.11 eV) and tends to have a smaller formation energy in the smaller L^{-1} (dilute) range as expected from extrapolation. This is an indication of the presence of $V(O_{ba})$ on this surface.

Such L^{-1} dependence is considered to arise from two main contributions to the defect formation energies; electrostatic and elastic contributions [11]. If a point defect with a charge q is treated by a periodic slab model, the charged defect suffers from electrostatic interactions with the defects in the periodic supercells, which results in L^{-1} (and higher order L^{-3} and others, in more detail) dependence of the defect formation energies [11]. In addition, atomic relaxation usually takes place around a point defect, and thus elastic interactions between point defects in the finite sized supercells also affect the defect formation energies. Since the present paper focuses on neutral charge states of the oxygen vacancies, the latter effect of atomic relaxation is expected to be responsible for the result in Fig. 2(a). As a matter of fact, the calculated formation energies tend to be smaller than those without atomic relaxation as shown in Fig. 2(b). In particular, it is evident that the formation energy of $V(O_{ba})$ is reduced by as large as about 2 eV by atomic relaxation. As can be seen in the calculated distances from the defects to neighboring atoms shown in Table I, it is found that the atomic relaxations over the second nearest neighbors (2NNs) of the bulk and bridging oxygen vacancies readily converge to less than a few percent. In the case of $V(O_{sub})$, one of the 1NN Ti (corresponding to Ti_{5c} above O_{sub}, see Fig. 1) moves outward by about 29% [at a distance of 2.48 Å from $V(O_{sub})$] to become the 2NN, but except for that, the atomic relaxations of 3NNs converge to less than several percent. In contrast, the basal oxygen vacancy shows the large inward relaxation of the 2NN oxygen atoms up to 11% as well as the outward relaxation of 1NN Ti of around 10%. The 2NN oxygen atom at a distance of 2.47 Å from O_{ba} becomes the 1NN around $V(O_{ba})$ (−8% relaxation) while the 3NN oxygen atoms also move toward the vacancy at a distance of 2.52 Å (−11% relaxation). It is observed that more atoms around $V(O_{ba})$ show the relatively large atomic relaxations of around 10%, even compared with the cases of other vacancies. Such larger atomic relaxations of $V(O_{ba})$ may be related to a larger reduction of the formation energy with atomic relaxation in Fig. 2(a) from the one without atomic relaxation in Fig. 2(b).

Since the comparable formation energy of $V(O_{ba})$ with $V(O_{br})$ is realized by using the rather large supercells, it is also important to investigate correspondence of the vacancy concentration in the supercells with the real surface environment. When one vacancy is produced on the surface in the 2×4 and 3×6 supercells, the apparent vacancy concentrations per surface correspond to 12.5% and 5.6%, respectively, which are very close to the experimental value of several percent [3,5]. It can be said, therefore, that the 3×6 supercell is reasonable to represent the real surface chemical environment and the comparative formation energy of $V(O_{ba})$ with $V(O_{br})$ obtained from the rather large supercells ensures existence of $V(O_{ba})$ on this surface, with the similar amount of $V(O_{br})$ at a relatively low coverage.

In order to further confirm the validity of the present result, it is also necessary to access effects of U parameters imposed on Ti $3d$ orbitals in the present GGA + U calculations. As stated by Morgan and Watson [17], the defect-induced level in the band gap and its spatial distribution due to the presence of $V(O_{br})$ on the (110) surface are affected by U parameters. Densities of states around the band gap for $V(O_{br})$ and $V(O_{ba})$ calculated with different U values of 0.0, 4.2, and 5.8 eV are investigated (see Fig. 3). In fact, energy positions of the defect-induced levels in the band gap are varied with U parameters. For $U = 4.2$ and 5.8 eV, the defect-induced levels appear in

TABLE I. Distance from oxygen vacancies to the neighboring atoms (in angstroms). These values are obtained from GGA + U calculations of the 3×6 surface supercells. Atomic species with the coordination numbers, the distances before relaxation, and the percentages of relaxation are displayed in parentheses.

	1NN	2NN	3NN
Bulk			
$V(O)$	2.14(2Ti, 2.01, +6.5%)	2.56(1O, 2.59, −1.2%)	2.82(4O, 2.86, −1.4%)
	2.22(1Ti, 2.03, +9.4%)		2.84(4O, 2.86, −0.7%)
Surface			
$V(O_{br})$	2.16(2Ti, 1.91, +13.1%)	2.55(1O, 2.58, −1.2%)	2.78(4O, 2.84, −2.1%)
$V(O_{ba})$	2.19(2Ti, 1.99, +10.1%)	2.52(2O, 2.84, −11.3%)	2.93(2O, 2.95, −0.7%)
	2.27(1O, 2.47, −8.1%)		2.96(2O, 2.97, ±0.0%)
	2.28(1Ti, 2.09, +9.1%)		
$V(O_{sub})$	2.13(2Ti, 2.05, +3.9%)	2.48(1Ti, 1.92, +29.2%)	2.78(4O, 2.83, −1.8%)
		2.59(1O, 2.59, ±0.0%)	3.00(4O, 2.95, +1.7%)

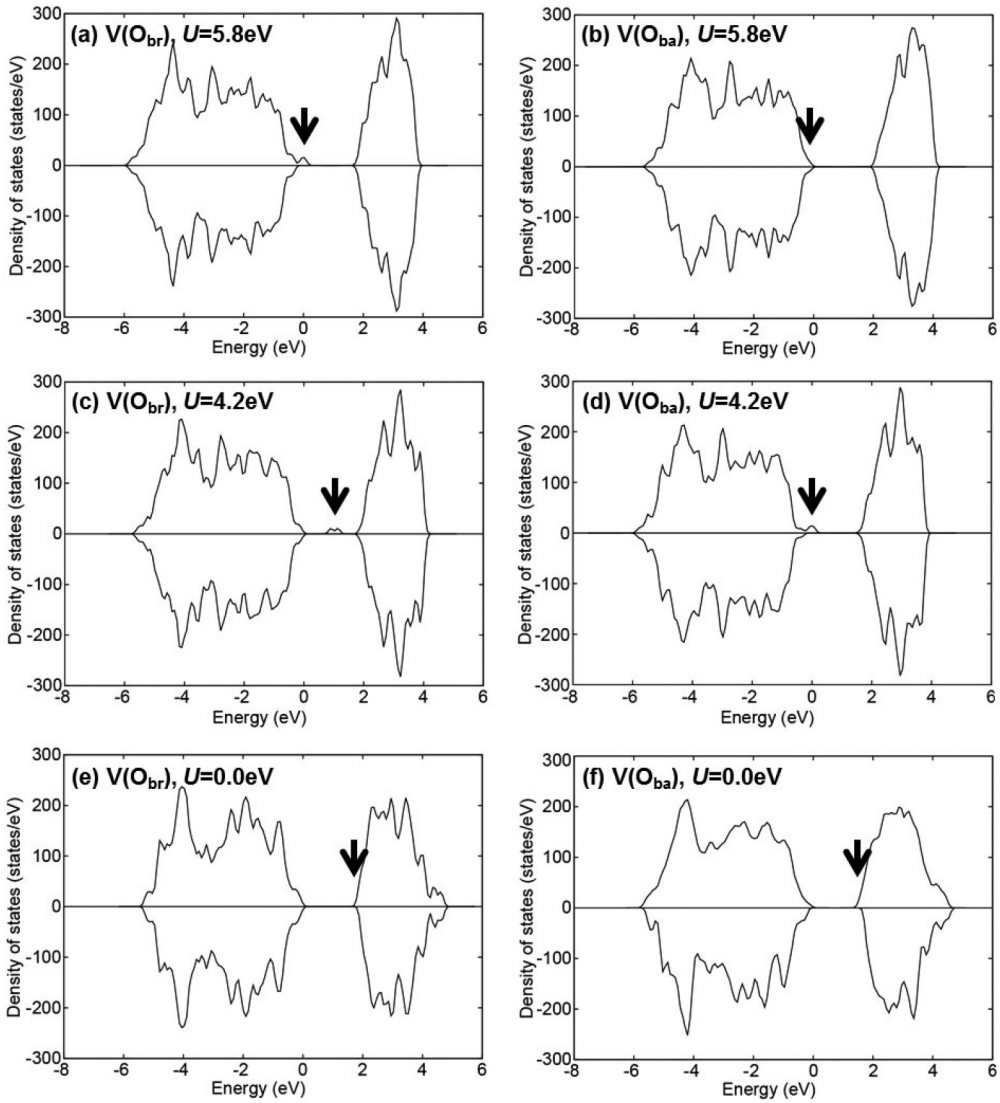

FIG. 3. Densities of states around the band gap for $V(O_{br})$ and $V(O_{ba})$, obtained from 2×4 supercells. The tops of the valence bands are set at 0 eV. For comparison, the results with different U parameters for Ti $3d$ are shown. The plots in (e) and (f) correspond to results obtained by normal GGA calculations without U correction. Arrows in the plots indicate positions of the highest electron-occupied levels.

the band gap and tend to be shifted higher in energy for the smaller U values.

In contrast, the defect-induced levels are not observed in the band gap explicitly for $U = 0.0$ eV (normal GGA calculations), and excess electrons of both $V(O_{br})$ and $V(O_{ba})$ are located at the bottom of the conduction band (see Fig. 3). Since it was experimentally reported that reduction of this surface produces extra states in the band gap, the electronic structures by the GGA + U calculations are more reasonable than those by the normal GGA ones [21]. Such a limitation of GGA for the surface electronic structure of TiO_2(110) was already discussed previously [12]. The correction of self-interaction error for the localized d states is important to describe the electronic structures of the surface oxygen vacancies in TiO_2. It is also noted that Cai *et al.* [22] recently reported the electronic structure of the bridging oxygen vacancy on TiO_2 (110) obtained by hybrid functional calculations. They showed that the bridging oxygen vacancy induces the defect states locating at 0.8 and 1.4 eV below the conduction band, which is in good agreement with our results, especially the one by $U = 4.2$ eV.

Such a difference in the electronic structures between GGA and GGA + U may also lead to a different behavior of the defect formation energies against L^{-1}. For GGA + U calculations, it can be seen in Fig. 4 that the formation energies of the vacancies increase by at most about 1 eV with the smaller U value. Although the energy positions of the defect-induced levels by $U = 4.2$ eV are in more reasonable agreement with experiment and hybrid functional calculations, the relative stability of the oxygen vacancies is not affected by the U values. Unlike the GGA + U case, however, the formation energies by GGA calculations shown in Fig. 5(a) tend to decrease with smaller L^{-1}, and $V(O_{br})$ is most stable over the entire range of L^{-1} in the GGA results. This can be expected because previous GGA calculations always predict the most stable defect species of $V(O_{br})$ on the surface. The difference in formation energy between $V(O_{br})$ and $V(O_{ba})$ is 1.2 eV in the 2×4 supercell of the present paper, which is in good

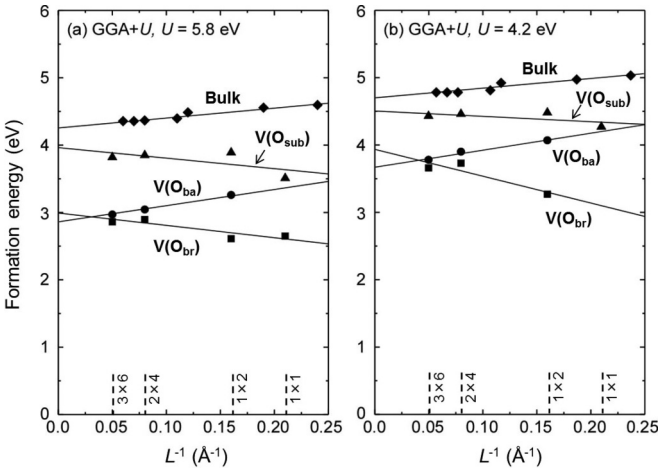

FIG. 4. Calculated formation energies of neutral oxygen vacancies by GGA + U with two different U parameters against the inverse of average interdefect distance L^{-1}.

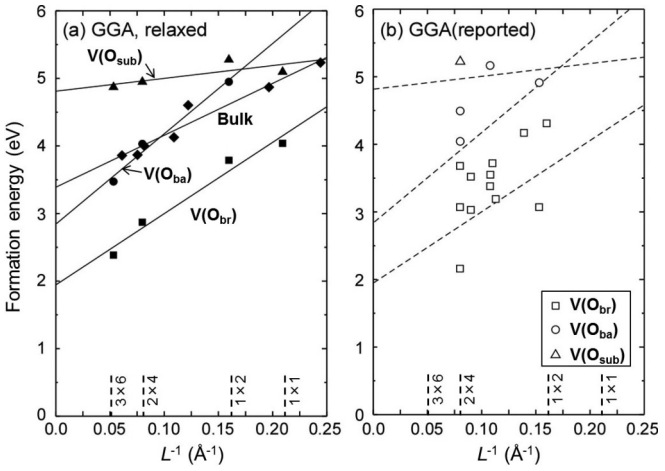

FIG. 5. (a) Calculated formation energies of neutral oxygen vacancies by GGA against an inverse of average interdefect distance L^{-1}. (b) Available previous GGA results plotted against L^{-1}. The three broken lines in (b) are identical with the least-square fitted lines for formation energies of $V(O_{br})$, $V(O_{ba})$, and $V(O_{sub})$ by GGA [shown in (a)], which are drawn as guides for the eye.

agreement with previous GGA results obtained by the similar 2×4 supercells with different slab thicknesses (0.98 eV by Kowalski *et al.* [19], and 0.82 eV by Cheng and Selloni [20]).

Previous GGA calculations with differently sized slab models for the oxygen vacancies on the TiO_2 (110) surface are summarized in Fig. 5(b) [17,19,20,23–26]. Although other detailed computational settings such as pseudopotentials, slab thicknesses and exchange-correlation functionals are different depending on previous GGA calculations, the reported GGA results are here plotted against L^{-1} estimated from the lateral sizes of the supercells used. Since the formation energies by GGA reported previously are scattered, it is difficult to make a quantitative comparison with the present result in Fig. 5(a). However, it is obvious that, as a whole, formation of $V(O_{br})$ is energetically more favorable than that of $V(O_{ba})$ and $V(O_{sub})$, irrespective of L^{-1}. It is confirmed, therefore, that GGA calculations cannot predict formation of $V(O_{ba})$ on the surface, and the correction of self-interaction error for Ti $3d$ in this case plays an important role for correctly evaluating the relative stability of $V(O_{ba})$ and $V(O_{br})$.

Our finding of the existence of the basal oxygen vacancy is likely related to the properties of the TiO_2 (110) surface. Such vacancies may work for an anchoring and binding site of metal atoms, clusters, and molecules. As a final note, our recent separate experimental study of atomic Pt adsorption on TiO_2 (110) demonstrates the presence of $V(O_{ba})$ to explain the most stable attachment site of Pt [27]. Therefore, this type of oxygen vacancy should become a clue to understanding the peculiar chemical activity of the TiO_2 surfaces, although they have not been explicitly remarked on so far. Further experimental investigations are expected to verify the presence of the new type of surface defect in TiO_2.

This study was supported by a Grant-in-Aid for Scientific Research on Innovative Areas "Nano Informatics" (Grants No. 25106002 and No. 25106003) from the Japan Society for the Promotion of Science (JSPS).

[1] U. Diebold, Surf. Sci. Rep. **48**, 53 (2003).
[2] M. V. Ganduglia-Pirovano, A. Hofmann, and J. Sauer, Surf. Sci. Rep. **62**, 219 (2007).
[3] C. L. Pang, R. Lindsay, and G. Thornton, Chem. Rev. **113**, 3887 (2013).
[4] N. Shibata, A. Goto, K. Matsunaga, T. Mizoguchi, S.D. Findlay, T. Yamamoto, and Y. Ikuhara, Phys. Rev. Lett. **102**, 136105 (2009).
[5] M. A. Henderson, Surf. Sci. **355**, 151 (1996).
[6] E. Wahlström, N. Lopez, R. Schaub, P. Thostrup, A. Rønnau, C. Africh, E. Lægsgaard, J. K. Nørskov, and F. Besenbacher, Phys. Rev. Lett. **90**, 026101 (2003).
[7] D. Matthey, J. G. Wang, S. Went, J. Matthiesen, R. Schaub, E. Lægsgaard, B. Hammer, and F. Besenbacher, Science **315**, 1692 (2007).
[8] P. J. D. Lindan, N. M. Harrison, and M. J. Gillan, Phys. Rev. Lett. **80**, 762 (1998).
[9] R. Schaub, P. Thostrup, N. Lopez, E. Lægsgaard, I. Stensgaard, J. K. Norskov, and F. Besenbacher, Phys. Rev. Lett. **87**, 266104 (2001).
[10] U. Diebold, J. Lehman, T. Mahmoud, M. Kuhn, G. Leonardelli, W. Hebenstreit, M. Schmid, and P. Verga, Surf. Sci. **411**, 137 (1998).
[11] G. Makov and M. C. Payne, Phys. Rev. B **51**, 4014 (1995).
[12] C. Di Valentin, G. Pacchioni, and A. Selloni, Phys. Rev. Lett. **97**, 166803 (2006).
[13] P. E. Blöchl, Phys. Rev. B **50**, 17953 (1994).
[14] G. Kresse and D. Joubert, Phys. Rev. B **59**, 1758 (1999).
[15] J. P. Perdew, K. Burke, and M. Ernzerhof, Phys. Rev. Lett. **77**, 3865 (1996).

[16] K. Yang, Y. Dai, B. Huang, and Y. P. Feng, Phys. Rev. B **81**, 033202 (2010).
[17] B. Morgan and G. W. Watson, Surf. Sci. **601**, 5034 (2007).
[18] L. A. Harris and A. A. Quong, Phys. Rev. Lett. **93**, 086105 (2004).
[19] P. M. Kowalski, B. Meyer, and D. Marx, Phys. Rev. B **79**, 115410 (2009).
[20] H. Cheng and A. Selloni, Phys. Rev. B **79**, 092101 (2009).
[21] V. E. Henrich, G. Dresselhaus, and H. Z. Zeiger, Phys. Rev. Lett. **36**, 1335 (1976).
[22] Y. Cai, Z. Bai, S. Chintalapati, Q. Zeng, and Y. Ping Feng, J. Chem. Phys. **138**, 154711 (2013).
[23] X. Wu, A. Selloni, and S. K. Nayak, J. Chem. Phys. **120**, 4512 (2004).
[24] J. Oviedo, M. A. SanMiguel, and J. F. Sanz, J. Chem. Phys. **121**, 7427 (2004).
[25] M. D. Rasmussen, L.M. Molina, and B. Hammer, J. Chem. Phys. **120**, 988 (2004).
[26] J. Graciani, L. J. Álvarez, J. A. Rodriguez, and J. F. Sanz, J. Phys. Chem. C **112**, 2624 (2008).
[27] T. Y. Chang, Y. Tanaka, R. Ishikawa, K. Toyoura, K. Matsunaga, Y. Ikuhara, and N. Shibata, Nano Lett. **14**, 134 (2014).